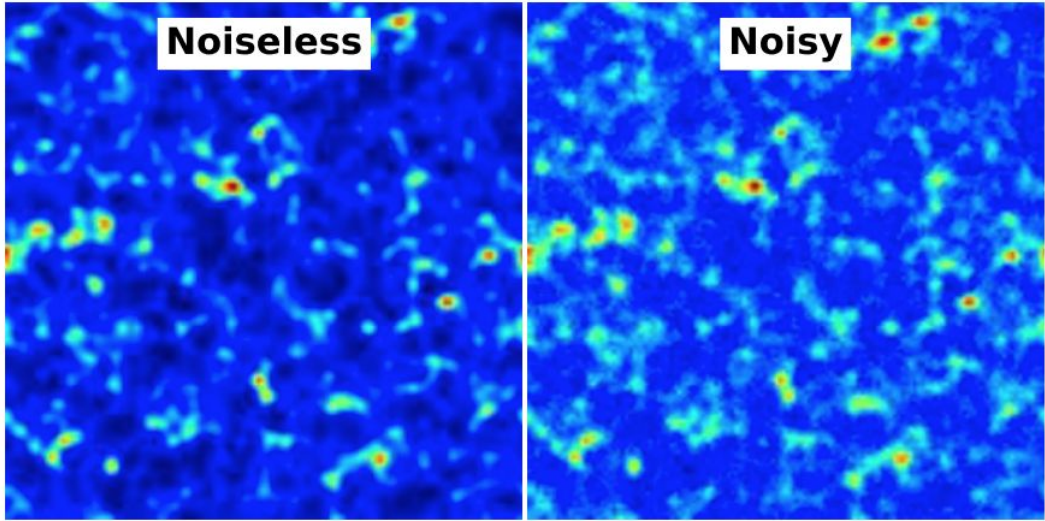


Title:	The Crab Pulsar at Centimeter Wavelengths II: Single Pulses
arXiv:	arXiv:1608.08881
Figure:	<p>The figure consists of two vertically stacked panels sharing a common x-axis representing Time in Microseconds, ranging from 0 to 5. The top panel is a line plot showing Intensity in Jy on the y-axis, ranging from 0 to 200. It displays a single pulse profile with a peak intensity of approximately 200 Jy occurring at about 2.2 microseconds. The bottom panel is a dynamic spectrum showing Frequency in GHz on the y-axis, ranging from 41 to 45 GHz. The intensity is represented by a color map where colors range from black (0 kJy) to red/yellow (2 kJy), as indicated by the color bar on the right. The dynamic spectrum shows a dispersive structure, with the pulse energy concentrated between 42.5 and 44.5 GHz and spreading out in time as frequency decreases. Overlaid on the color map are grey contour lines representing intensity levels of 0.2, 0.5, 1, and 2 kJy. An orange line is also visible on the left side of the dynamic spectrum, likely representing the noise floor or a reference level.</p>
Caption:	<p>The total intensity of a Main Pulse recorded at 43.25 GHz and de-dispersed using DM of 56.794 pc-cm⁻³ (taken from Jodrell Bank monitoring for our observing date) is shown with a time resolution of 44.8 ns. The frequency resolution of the dynamic spectrum is 78 MHz. The Intensity contour levels in the dynamic spectrum are 0.2, 0.5, 1, and 2 kJy. The off-pulse noise level for the total intensity is 15.2 Jy, and for the dynamic spectrum, 110 Jy</p>

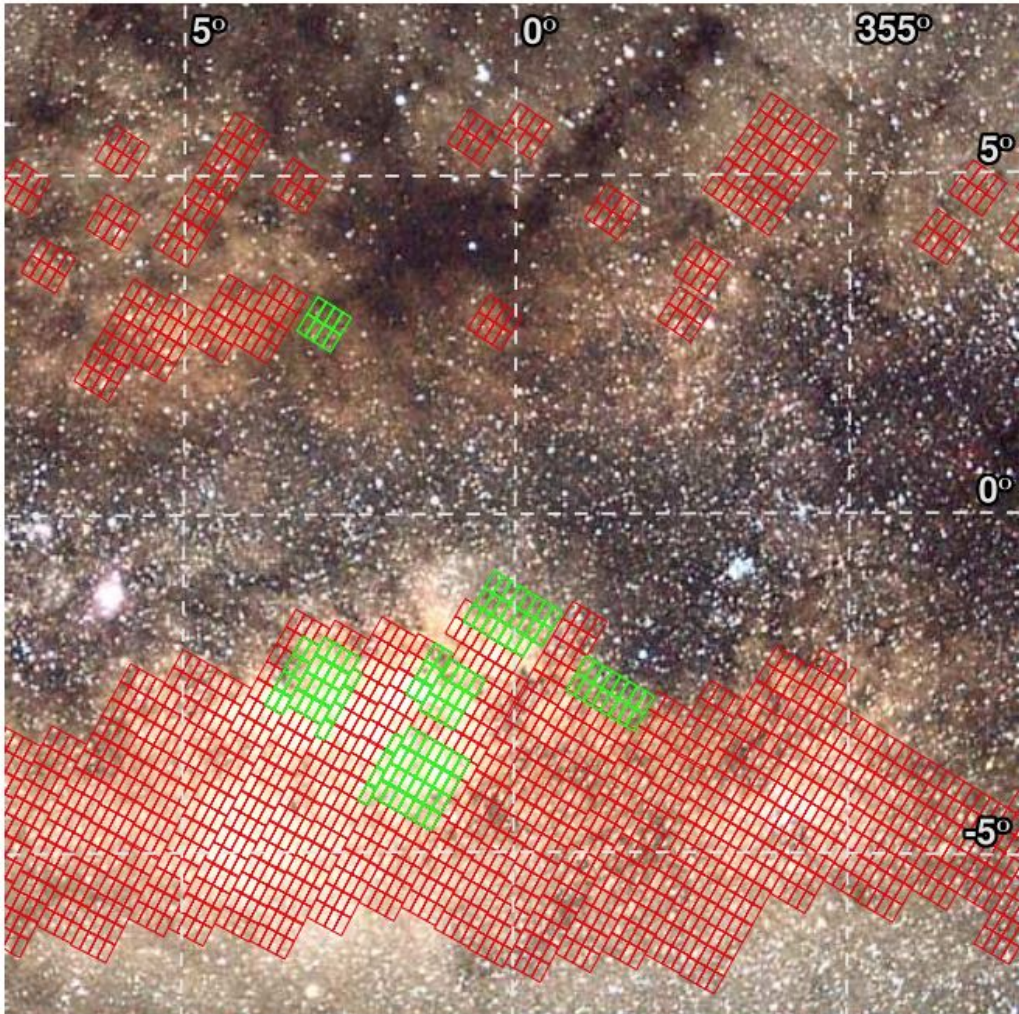
Title:	Towards optimal extraction of cosmological information from nonlinear data
arXiv:	arXiv:1706.06645
Figure:	
Caption:	The truth simulations without (left) and with (right) noise.

Title:	Merging Galaxies with Tidal Tails in COSMOS to $z=1$
arXiv:	arXiv:1608.04298
Figure:	<p>The figure consists of four panels arranged in a 2x2 grid, each showing the relationship between the color index $U-V$ (y-axis) and $V-J$ (x-axis) for galaxies in different redshift bins. The panels are labeled with their respective redshift ranges: $0.2 \leq z < 0.4$, $0.4 \leq z < 0.6$, $0.6 \leq z < 0.8$, and $0.8 \leq z < 1$. Each panel contains a large number of gray points representing the parent sample of 35,076 galaxies. Overlaid on these are black circles representing merging galaxies containing tidal dwarf galaxy (TDG) candidates, and green circles representing merging galaxies with long tidal tails. Solid lines in each panel indicate the adopted division between quiescent galaxies (above the line) and star-forming galaxies (below the line). A legend in the top-left panel identifies the symbols: black circle for 'gal. with TDG' and green circle for 'gal. with long tail'.</p>
Caption:	<p>The $U - V$ Vs. $V - J$ diagram of 461 merging galaxies with long tidal tails (solid circles) in comparison with the parent sample of 35 076 galaxies (gray points). The black (green) circles represent mergers containing (or not) tidal dwarf galaxy candidates. The solid lines show the adopted division between the star-forming and quiescent galaxies in each redshift bin.</p>

Title:	Interacting galaxies: co-rotating and counter-rotating systems with tidal tails
arXiv:	arXiv:1312.0560
Figure:	<p>The figure consists of six histograms arranged in a 3x2 grid. The left column represents the 'Galaxies' sample, and the right column represents the 'AGN' sample. The rows represent different physical properties: redshift (z), absolute r-band magnitude ($\log(M_r)$), and stellar mass (M_r). Each histogram compares co-rotating pairs (solid blue line) and counter-rotating pairs (dotted red line). The y-axis for all plots is frequency (f).</p> <ul style="list-style-type: none"> Top Row (Redshift z): The x-axis ranges from 0 to 0.1. Co-rotating pairs peak at $z \approx 0.06$, while counter-rotating pairs peak at $z \approx 0.04$. Middle Row (Absolute Magnitude $\log(M_r)$): The x-axis ranges from 9 to 11.5. Co-rotating pairs peak at $\log(M_r) \approx 10.5$, while counter-rotating pairs peak at $\log(M_r) \approx 10.2$. Bottom Row (Stellar Mass M_r): The x-axis ranges from -18 to -23. Co-rotating pairs peak at $M_r \approx -20.5$, while counter-rotating pairs peak at $M_r \approx -20.2$.
Caption:	<p>Distribution of redshift (top), absolute r-band magnitude (middle) and stellar mass content (bottom) for the non-AGN galaxy sample (left) and for the AGN galaxy sample (right) in co and counter-rotating pairs. The solid lines correspond to the co-rotating and the dotted lines correspond to the counter rotating galaxy pairs, respectively.</p>

Title:	OMEGA - OSIRIS Mapping of Emission-line Galaxies in A901/2: III. - Galaxy Properties Across Projected Phase Space in A901/2
arXiv:	arXiv:1706.05199
Figure:	<p>The figure consists of three panels. The left panel is a histogram of the difference between prism and spectroscopic redshifts, $z_{\text{prism}} - z_{\text{2dF,VIMOS}}$, with a median offset of -0.004. The middle panel is a scatter plot of $z_{\text{2dF,VIMOS}}$ versus z_{prism} for $z_{\text{prism}} \geq 0.12$ (N=143), showing a linear fit $y = 0.65x + 0.06$. The right panel shows the same data after correction, with the prism redshifts recalibrated to better match the spectroscopic redshifts.</p>
Caption:	<p>This figure compares the spectroscopic and prism redshifts for a subset of 143 galaxies having both kinds of redshifts. The left panel shows the distribution of offsets between the spectroscopic and prism redshifts. The middle panel shows that the offset is redshift dependent. The solid line is $y = x$. The dashed line is a fit to the data. In the right panel, we have used the fit from the middle panel to recalibrate the prism redshifts to better match the spectroscopic redshifts.</p>

Title:	OMEGA - OSIRIS Mapping of Emission-line Galaxies in A901/2: III. - Galaxy Properties Across Projected Phase Space in A901/2
arXiv:	arXiv:1706.05199
Figure:	<p>The figure is a scatter plot of galaxy positions in Right Ascension (RA) and Declination (DEC). The RA axis ranges from 148.80 to 149.40, and the DEC axis ranges from -10.3 to -9.7. The plot shows a dense distribution of galaxies, categorized by their source: Vimos/AAT (blue diamonds, N=359), OMEGA (green squares, N=273), and Prism (red circles, N=224). Four subclusters are highlighted with black triangle markers and labeled in the legend: A901a (top center), A901b (top left), A902 (top right), and the SW Group (bottom left). Each subcluster is enclosed by a black circle representing its sphere of influence (R200).</p>
Caption:	The top panel shows the spatial distribution of the 856 galaxies in sample S2 coded by the source of the adopted redshifts. The four subclusters are separately labelled, and their spheres of influence (R200) are shown as circles.

Title:	Interstellar extinction curve variations towards the inner Milky Way: a challenge to observational cosmology
arXiv:	arXiv:1510.01321
Figure:	
Caption:	<p>Subset of OGLE-III subfields shown in red overlaid on an optical image of the Galactic bulge with Galactic coordinate system shown as well. The subfields used in this work, for which we also use the matching V V V photometry, are shown in green.</p>

Title:	Ages of Type Ia supernovae over cosmic time
arXiv:	arXiv:1409.2951
Figure:	<p>The figure consists of three side-by-side contour plots. All three plots share the same axes: the x-axis is 'Galaxy Stellar Mass' ranging from 8 to 12, and the y-axis is 'Stellar Age' ranging from 0 to 12. The left plot, titled 'Normalized Galaxy SFHs', shows a broad distribution of stellar ages across the mass range. The middle plot, titled 'SN Ia Age Distributions', shows a similar but more concentrated distribution. The right plot, titled 'Final SN Ia Number Density', shows a distinct peak in density at higher stellar masses and younger ages, with a secondary peak at lower masses and older ages.</p>
Caption:	<p>Left: Normalized mean galaxy SFHs as a function of total stellar mass. Middle: SN Ia age distribution versus host galaxy mass (not re-normalized: age distribution per unit mass). Right: Intrinsic distribution of SNe Ia in progenitor age-host mass space in the local Universe ($z = 0$).</p>

Title:	Linking the structural properties of galaxies and their star formation histories with STAGES
arXiv:	arXiv:1510.01115
Figure:	<p>The figure consists of four panels, each representing a different galaxy morphology: E (Elliptical), S0, Sp (Spiral), and Irr (Irregular). Each panel contains a scatter plot of $\log(\text{SSFR yr}^{-1})$ versus $\Delta(W_{462} - W_{518})$ and two histograms. The scatter plots show data points for relaxed systems (black squares), disturbed galaxies (blue circles), and visual mergers (red symbols). Plus signs represent objects with only SFR upper or lower limits. The histograms show the distribution of SSFR (left) and $\Delta(W_{462} - W_{518})$ (right). The SSFR histogram excludes objects with only SFR upper or lower limits. The $\Delta(W_{462} - W_{518})$ histogram includes all objects. The histograms are normalized to a maximum value of one to amplify differences between the distribution functions.</p>
Caption:	<p>Specific SFR vs. $\Delta(W_{462} - W_{518})$ for cluster galaxies of all morphologies. As in Fig. 2, black squares correspond to relaxed systems, blue circles to disturbed galaxies not classified as mergers and red symbols to visual mergers. Objects with only SFR upper or lower limits are presented as pluses with appropriate colours. In the accompanying histograms, the black dashed line shows the relaxed galaxies, the blue solid line the disturbed ones, and the red histogram the visual mergers. The SSFR histogram excludes objects with only SFR upper or lower limits. The $\Delta(W_{462} - W_{518})$ histogram includes all objects. In all cases, the histograms are normalized to a maximum value of one in order to amplify the differences between the distribution functions.</p>

Title:	The 2-degree Field Lensing Survey: design and clustering measurements
arXiv:	arXiv:1608.02668
Figure:	<p>The figure displays a series of stacked spectra for Luminous Red Galaxies (LRGs) from the 2-degree Field Lensing Survey (2dFLenS). The spectra are arranged vertically, corresponding to redshift slices from $z=0.05$ at the top to $z=0.95$ at the bottom. The x-axis represents the rest-frame wavelength in Angstroms (\AA), ranging from 3000 to 7000. The y-axis represents the flux, which is offset for each spectrum to allow for comparison. Vertical dotted lines are drawn across the spectra to highlight specific spectral features that are common across the redshift range. These features are labeled at the top: $[\text{MgII}]$ (around 3480 \AA), $[\text{OII}]$ (around 3727 \AA), $\text{KHH}\delta$ (around 3970 \AA), $\text{GH}\gamma$ (around 4101 \AA), $\text{H}\beta/[\text{OII}]\text{Mg}$ (around 4831 \AA), Na (around 5890 \AA), and $\text{H}\alpha/[\text{NII}]$ (around 6563 \AA). The spectra show a general trend of decreasing flux with increasing wavelength, with the most significant absorption features appearing in the blue/UV part of the spectrum.</p>
Caption:	Spectra of 2dFLenS LRGs with good-quality redshifts stacked by rest-frame wavelength in $\Delta z = 0.1$ slices. Prominent spectral features are indicated by the vertical dotted lines.